Mathematical Modeling, Laboratory Testing and Numerical Simulation of a Servo-Pump as Part of a Closed Circuit Primary Control Hydrostatic Transmission for Multi-Purpose Trucks

PhD. Stud. Eng. **Alexandru-Polifron CHIRIȚĂ**[1,2,*], Prof. PhD. Eng. **Cristian PAVEL**[1]

[1] Technical University of Civil Engineering of Bucharest (UTCB), Faculty of Technological Equipment, Bucharest, Romania

[2] National Institute of Research & Development for Optoelectronics / INOE 2000 – Subsidiary Hydraulics and Pneumatics Research Institute / IHP, Bucharest, Romania

* chirita.ihp@fluidas.ro

Abstract: *The current paper presents the dynamic mathematical models of the components of a hydrostatic transmission, the results of physical tests performed in the laboratory on a servo-pump that is part of a closed circuit primary control hydrostatic transmission, and its numerical simulation results. The acquisition of the experimental data as well as the control of the experimental stand have been carried out with the LabVIEW application, while the numerical simulation has been carried out by using the AMESim software; in order for the results of the numerical simulation to be as close as possible to those obtained in the laboratory, the library of hydraulic components that take into account the influence of temperature on the hydraulic fluid and on the hydraulic components of the transmission has been used.*

Keywords: *Mathematical modeling, laboratory testing, numerical simulation, closed circuit, primary control, hydrostatic transmission, servo-pump*

1. Introduction

In hydraulic transmissions, power is transmitted through a fluid; it connects the pump to the hydrostatic motor [1]. The hydraulic pump receives mechanical energy from the internal combustion engine or the electric one and transfers it to the fluid in the form of flow and pressure (hydraulic energy) [2]. The fluid carries the hydraulic energy to the hydraulic motor where it is converted back into mechanical energy [1, 3].
The basic elements of a hydraulic transmission are: the pump, the fluid and the motor. They have the following roles [4, 5]:
• The pump transforms mechanical energy into hydraulic energy;
• The fluid carries the hydraulic energy from the pump to the motor;
• The motor converts hydraulic energy into mechanical energy.
Hydrostatic transmissions involve connecting a positive displacement pump to a positive displacement motor [3]. In this case, the pump produces the flow that turns the motor shaft, and the pressure in the circuit is produced by the torque resisting the motor shaft [1, 4].
Closed loop transmissions have both pump and motor ports connected together. The discharge port of the pump is connected to the "A" port of the motor and the "B" port of the motor is connected to the suction of the pump [6].
In a closed circuit hydrostatic transmission there are three ways of controlling the speed of the hydraulic motor shaft [3]:
• Primary control – when the pump displacement is variable.
• Secondary control – when the hydrostatic motor displacement is variable;
• Mixed control – when both pump and motor displacement are variable.
In the first of the cases listed above, that is, primary control, when the pump flow rate is variable and depends on the variation of the pump displacement, and the motor displacement is fixed, the motor speed is directly proportional to the flow rate delivered by the pump to the hydraulic motor port [6, 7]. In this particular case, the torque produced at the motor shaft is constant over the entire motor speed range [8] - from minimum speed rate to maximum speed rate - and the pressure created in the system is proportional to the torque. This is the most popular configuration [4, 6] and

is used because the transmission ratio is infinitely variable. Moreover, the reversal of the direction of rotation of the motor is achieved without shocks and continuously [9, 10, 11].
The mathematical models related to the main components of a hydrostatic transmission are presented below as follows:
The dynamic mathematical model and an illustration of a pump are presented in Fig. 1; Fig. 2 shows the dynamic mathematical model of a high-speed hydrostatic motor; Fig. 3 - the dynamic mathematical model of a low-speed hydrostatic motor; and finally, Fig. 4 shows an illustration of a hydraulic cylinder as well as its dynamic mathematical model.

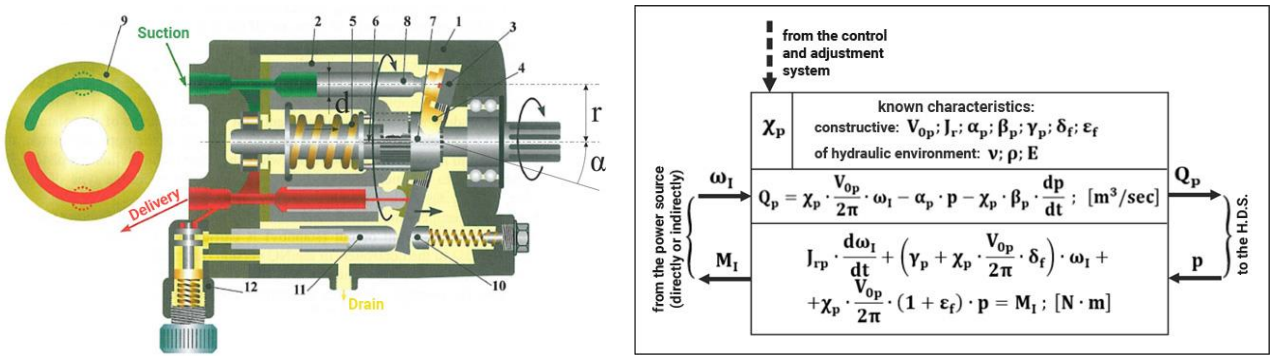

Fig. 1. Swash plate hydraulic pump and the dynamic mathematical model of the pump – adapted from [1] and [12]

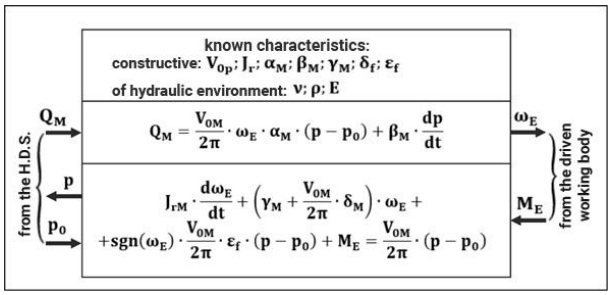

Fig. 2. Dynamic mathematical model of a high-speed fixed-displacement motor - adapted from [12]

$$Q_M = \left(\frac{V_{0M}}{2\pi} - k^*\right) \cdot \omega_e + \alpha_M^* \cdot p^2 + \beta_M \cdot \frac{dp}{dt};$$

$$J_{SM} \cdot \frac{d\omega_e}{dt} + \left(\frac{V_{0M}}{2\pi} - k^*\right) \cdot \delta_M^* (\omega_e - \omega_S)^2 + M_E = = \left(\frac{V_{0M}}{2\pi} - k^*\right) \cdot p;$$

$$\alpha_M^* = (\pi \cdot d \cdot z \cdot k \cdot j^3/96 \cdot b \cdot \eta) \cdot 2\pi \cdot d \cdot z \cdot k/\rho \cdot g \cdot V_{0M}$$

Fig. 3. Dynamic mathematical model of a low-speed radial piston motor - adapted from [12]

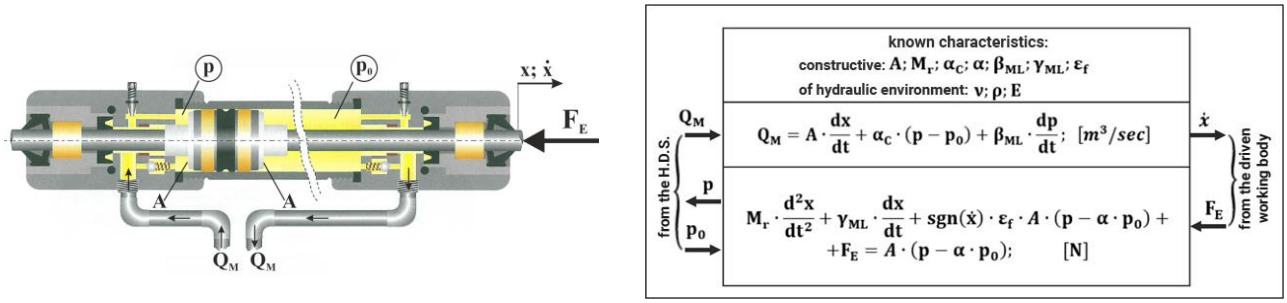

Fig. 4. Hydraulic cylinder and the dynamic mathematical model of a hydraulic cylinder – adapted from [1] and [12]

2. Material and method

This chapter is divided into two subchapters, the first of which deals with the methodology of physical experimentation, in the laboratory, and the second deals with the methodology of virtual experimentation with the help of numerical simulation.

2.1 Methodology of physical experimentation in the laboratory

The figures below show the experimental bench and its components. Experiments related to the adjustment characteristic and the response of the servo-pump to the step signal have been carried out on this bench.

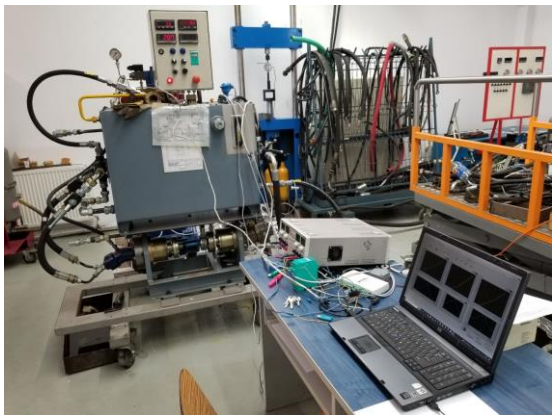

Fig. 5. The experimental test bench - front view

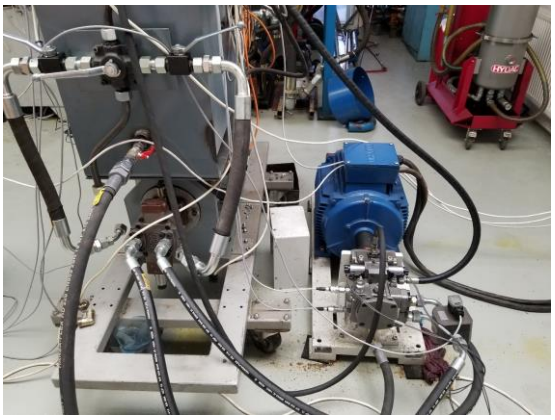

Fig. 6. The experimental test bench - side view

Fig. 7. The electric cabinet for the bench and electric motor control

As one can see in **Error! Reference source not found.**, **Error! Reference source not found.** and **Error! Reference source not found.**, the test bench consists of four distinct components:

- The first of these components is the **electric pump**, which has an asynchronous electric motor - with the power of 30 kW and the synchronism speed of 1500 rev/min – as one of its parts and the A10VG28 servo-pump;
- **Load simulation unit**, comprising: the hydraulic oil tank, the panel with digital displays for speed, temperature and torque, the A6VM servo-motor and the F112A fixed displacement pump;
- **Experimental data acquisition system**, consisting of a laptop equipped with LabVIEW experimental data acquisition software, NI 6211 experimental data acquisition board, various transducers and a programmable voltage source;
- **Electric cabinet for the bench and electric motor control**, shown in Fig. 7, with the following parts: 30-kW circuit breaker, star delta starter, 24 V power supply, 12 V power supply, 1P – 10 A automatic fuse, 3P – 1 A automatic fuse, IEM3255 three-phase meter with Modbus RTU communication and ±10 V proportional controller.

The hydraulic schematic diagram of the experimental test bench on which the research on the closed-circuit primary control hydrostatic transmission has been carried out is shown below, in Fig. 8.
Operation of the experimental test bench: one supplies the test bench with electricity and opens the LabVIEW application related to the experiment to be performed.

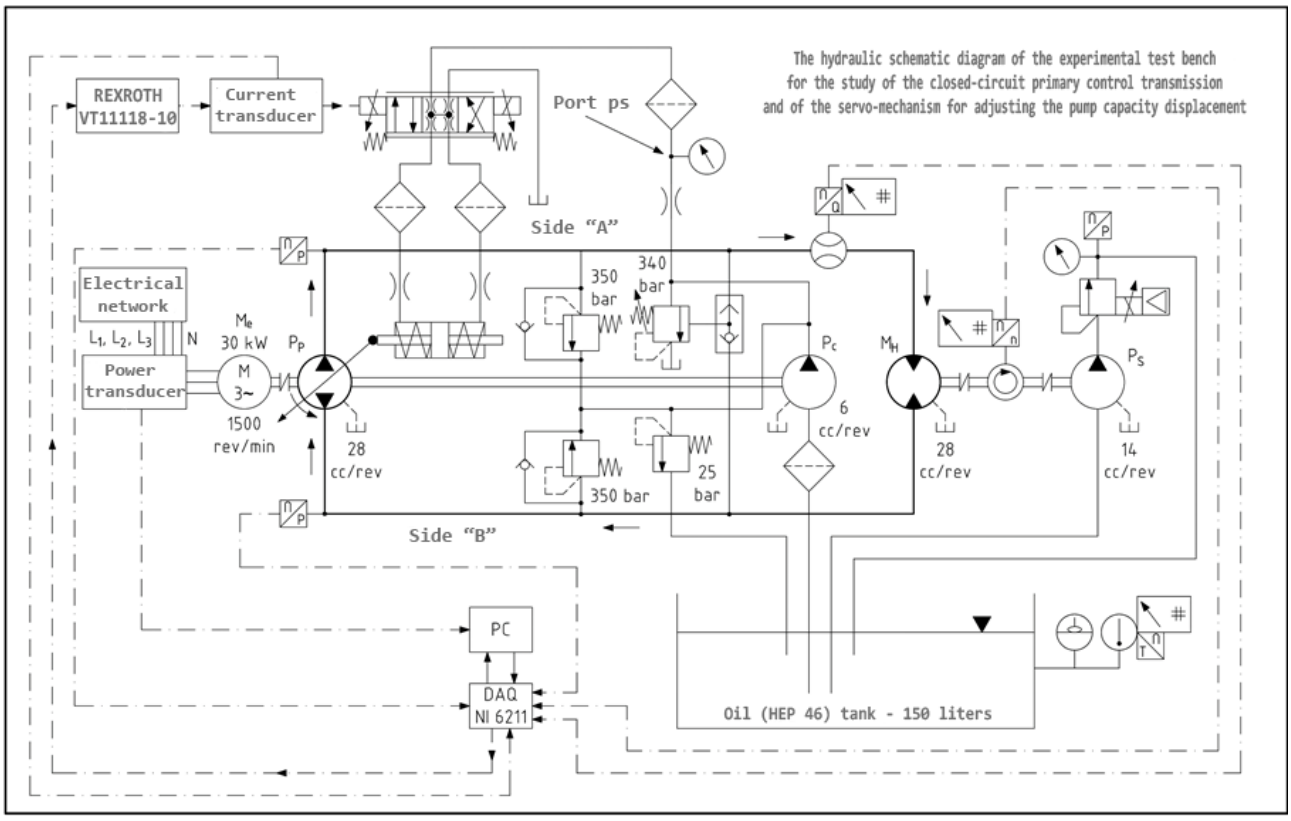

Fig. 8. Hydraulic schematic diagram of the experimental test bench for the study of the closed-circuit primary control transmission and the pump displacement control servo-mechanism

Notations in the hydraulic diagram: M_e – electric motor, P_P – main pump, P_c – compensation pump, M_H – hydrostatic motor, P_S – pressure gauge port, DAQ – experimental data acquisition board, PC – laptop and REXROTH VT11118-10 – signal conditioner for driving the pump servo-mechanism

From the electrical cabinet, the electric motor is turned on; one waits for it to switch from star to delta, and then presses the "start" button of the LabVIEW application. The control signal is transmitted from the PC to the experimental data acquisition board, which converts it to voltage (0 - 10 V); this voltage reaches the VT11118-10 proportional controller which conditions the signal and transforms it into the control current (0 – 600 mA) of the electromagnets of the proportional directional valve that is part of the pump displacement control servo-mechanism. The proportional directional valve controls the displacement of the hydraulic cylinder with bilateral rods; this displacement is directly proportional to the control signal, the swash plate angle, the main pump displacement, and its flow rate. After the swash plate angle exceeds the value of + 3º, the main pump discharges, on side "A", a flow of hydraulic fluid that passes through the flow transducer and reaches the hydrostatic motor; the flow rate determines the speed rate of the hydrostatic motor, which is measured by the speed transducer; this speed rate drives the load pump, whose flow is forced through the proportional pressure control valve, which creates a resisting torque on the motor shaft; this torque is proportional to the pressure reached at the pressure control valve. Given the ratio of the displacement of the hydrostatic motor to that of the load pump, when on the high-pressure side of the closed circuit the pressure is 70 bar, a pressure of 140 bar is installed at the proportional pressure control valve. The flow rate of the compensation pump, with a value of approximately 9 l/min at a pressure of 25 bar, provides the required flow rate to the servo-mechanism at a pressure of 20 bar, measured at port *ps*, compensates the volumetric losses of the pump with the help of check valves, and the rest of the flow drains to the tank through the pressure control valve set at 25 bar. The throttle between the compensation pump and the proportional directional control valve is meant to limit the pressure pulsations of the compensation pump that would reach the directional control valve. The throttles on the ports of the hydraulic cylinder have the role of equalizing its displacement speed and slowing the response of the servo-mechanism to

the control signal. The pressure control valves set at 350 bar act as safety valves, and the pressure control valve (set at 340 bar) which is controlled by the pressure in the closed circuit branches via the selector valve has the role of reducing the pump capacity if the pressure in the closed circuit exceeds the set value. The power transducer directly communicates to the PC the time-variation of the power absorbed by the electric motor, and the rest of the transducers transmit to the PC, by means of the experimental data acquisition board, signals proportional to the parameter values measured by them. After the data acquisition completion condition has been reached, the acquisition stops automatically; then the electric motor and the power supply to the bench are switched on; after performing these operations, the results of the experiment can be saved.

2.2 Methodology of virtual experimentation with numerical simulation

The initial data of the experimentation and those of the numerical simulation of the servo-pump are identical, including the control signal. In this subsection, the initial parameters of the components will be presented briefly.

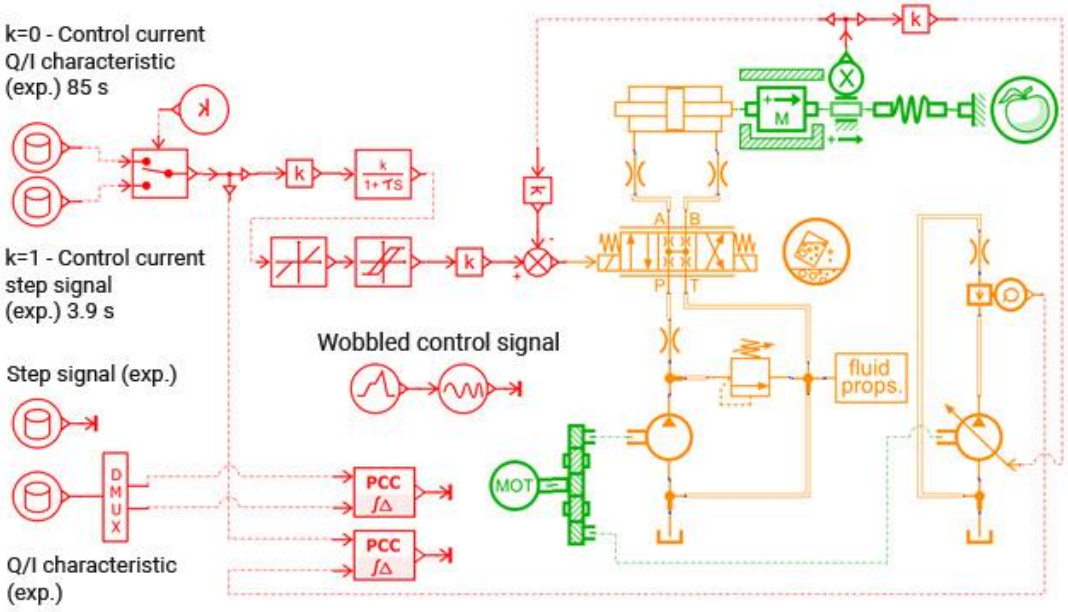

Fig. 9. Servo-pump simulation network

The servo-pump simulation network is presented in Fig. 9; on it, one can identify: in green colour - mechanical components, in red - electronic components or those carrying various signals, and in orange - hydraulic components, which also take thermal phenomena into account; without them, the results of the numerical simulation could not have been compared with the results of the laboratory experiments. The current control signal is the one determined experimentally; it passes through the electronic blocks, which condition it and send it to the servo-mechanism that controls the pump displacement volume (flow rate) proportional to the value of the control current. The main pump has a displacement of 28 cm^3/rev, and the compensation pump - a displacement of 6 cm^3/rev; the hydraulic fluid is ISO VG 46, and the pressure control valve is set at 20 bar.

3. Results

Just like the previous chapter, this chapter is divided into two subchapters, the first of which presents the results of physical experimentation and the second presents the results of virtual experimentation.

3.1 Results of physical experimentation in the laboratory

To be able to have an overview of the experiments in this section of the chapter and for an easier interpretation of the results of the experiments carried out, the experimental data related to the

servo-pump flow rate, measured with the flowmeter placed in the closed circuit, have been imported into MS. Excel. There, the four curves have been superimposed so that the lag shown in Figure 10 can be read on the "X" axis of the graph.

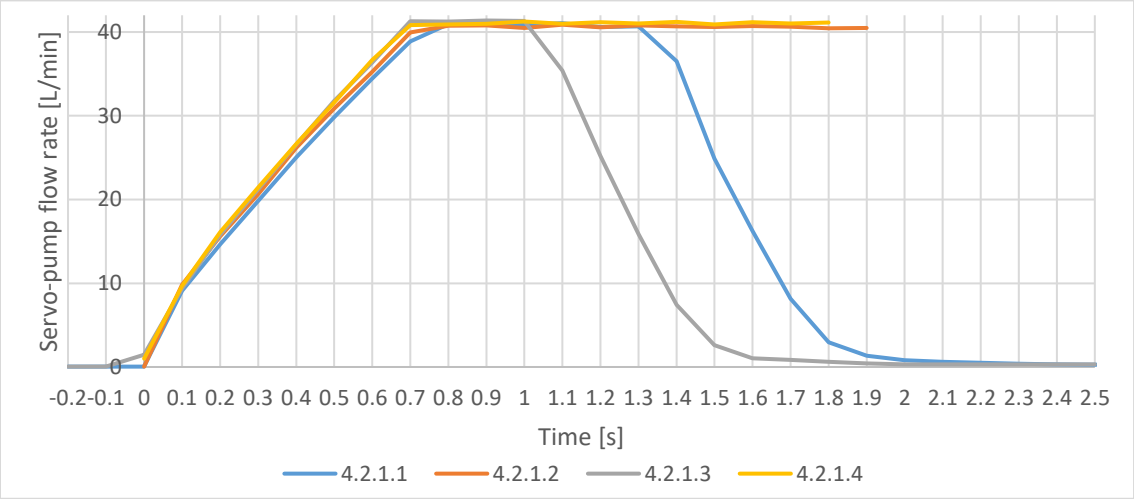

Fig. 10. Response to step signal – centralized results

On the panel of the application made in LabVIEW for the response to the step signal of the servo-pump - shown in Fig. 11, one can see the graphs for the following parameters that vary over time: the control current, the flow rate of the servo-pump, the control voltage, as well as the pressure on the two sides of the transmission.

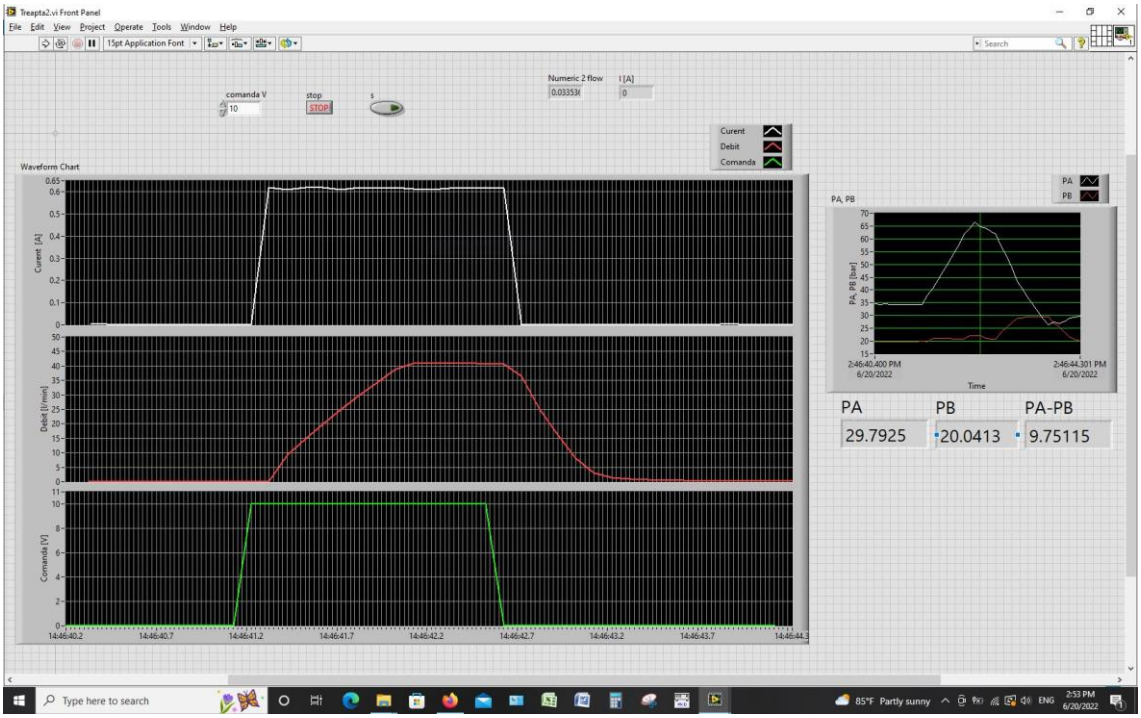

Fig. 11. Application panel – A10VG28EP4 servo-pump response to step signal

A10VG28EP4 servo-pump flow rate/control characteristic and transmission characteristic

The application panel related to the experimentation with load created by the hydrostatic motor and the maximum control signal is shown in Fig. 12, while for the minimum control signal the application panel is shown in Fig. 13. These panels contain pump and transmission characteristics

on the first row, and on the second row, as a function of time, there are shown variation of power absorbed by the electric motor, variation of the control current of the proportional directional valve in the servo-pump structure, and pressure variation on the sides of the closed circuit.

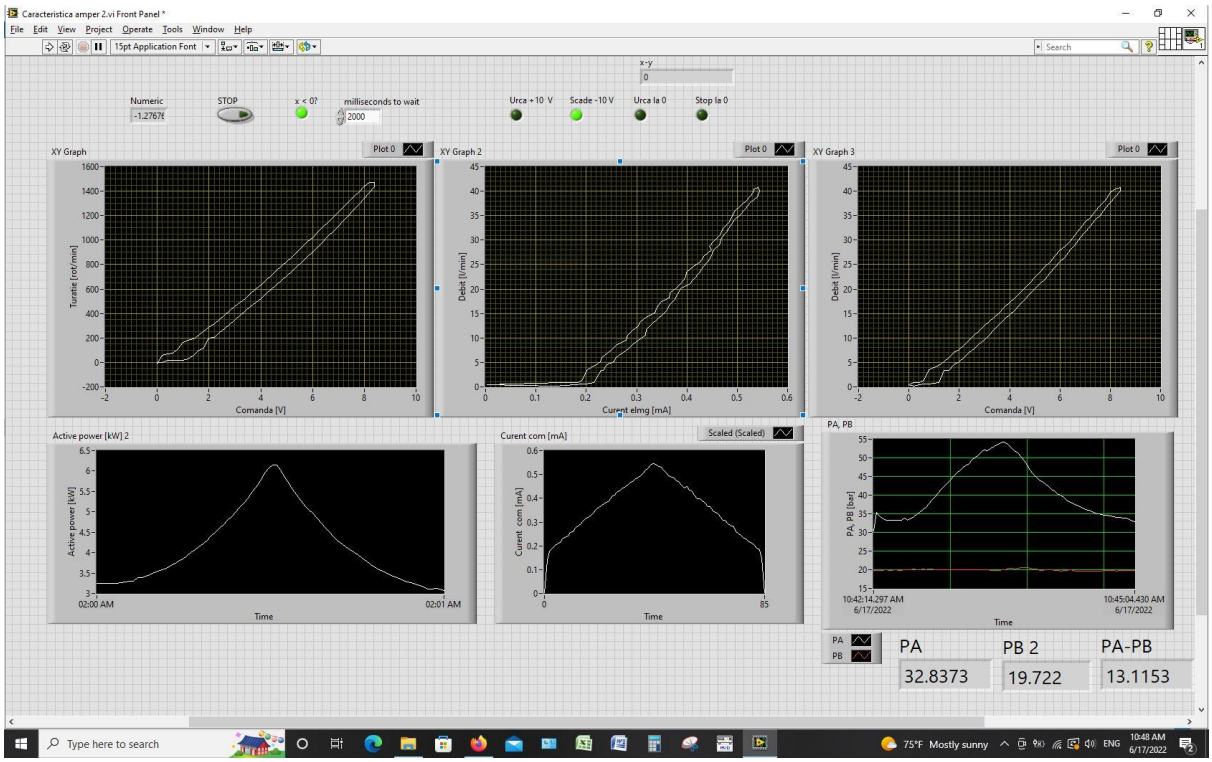

Fig. 12. Application panel related to the experimentation with load created by the hydrostatic motor and the maximum control signal

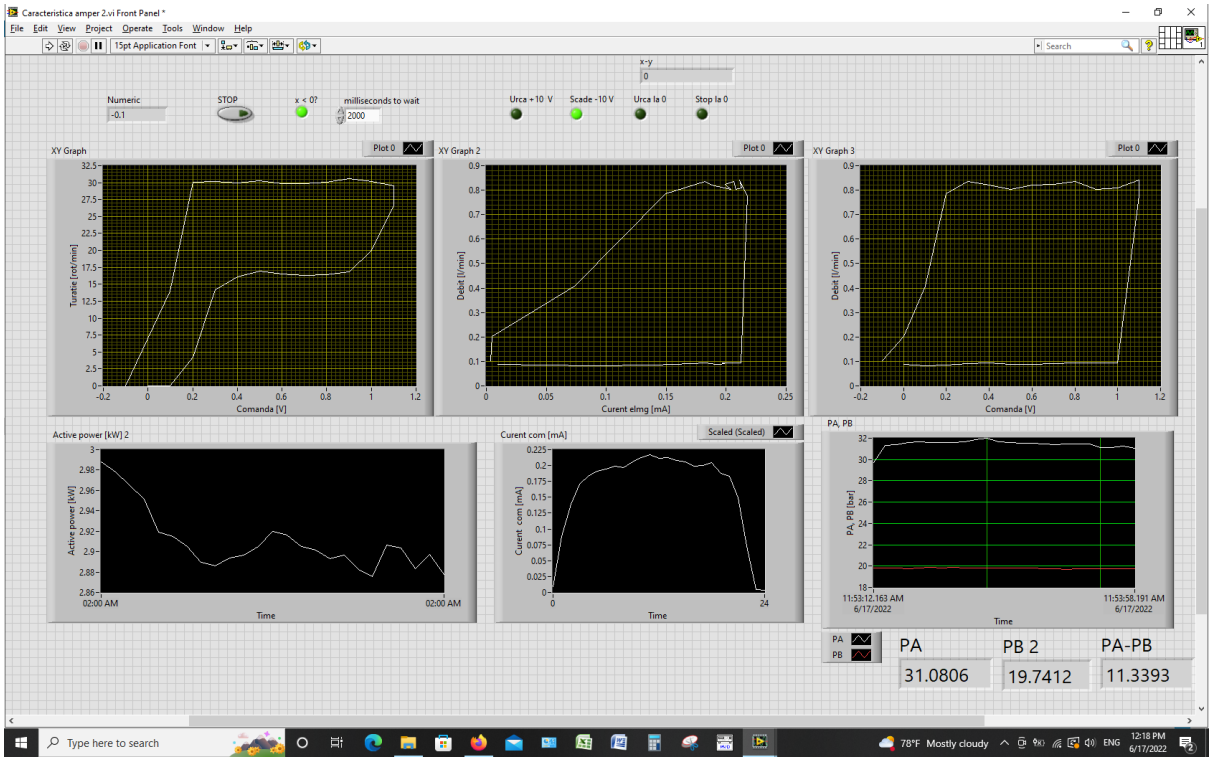

Fig. 13. Application panel related to the experimentation with load created by the hydrostatic motor and the minimum control signal

3.2 Results of virtual experimentation with numerical simulation

Servo-pump response to step signal

In Fig. 14 one can see that the time-variation of the simulated servo-pump flow rate is almost identical to the experimental one; the control current is common.

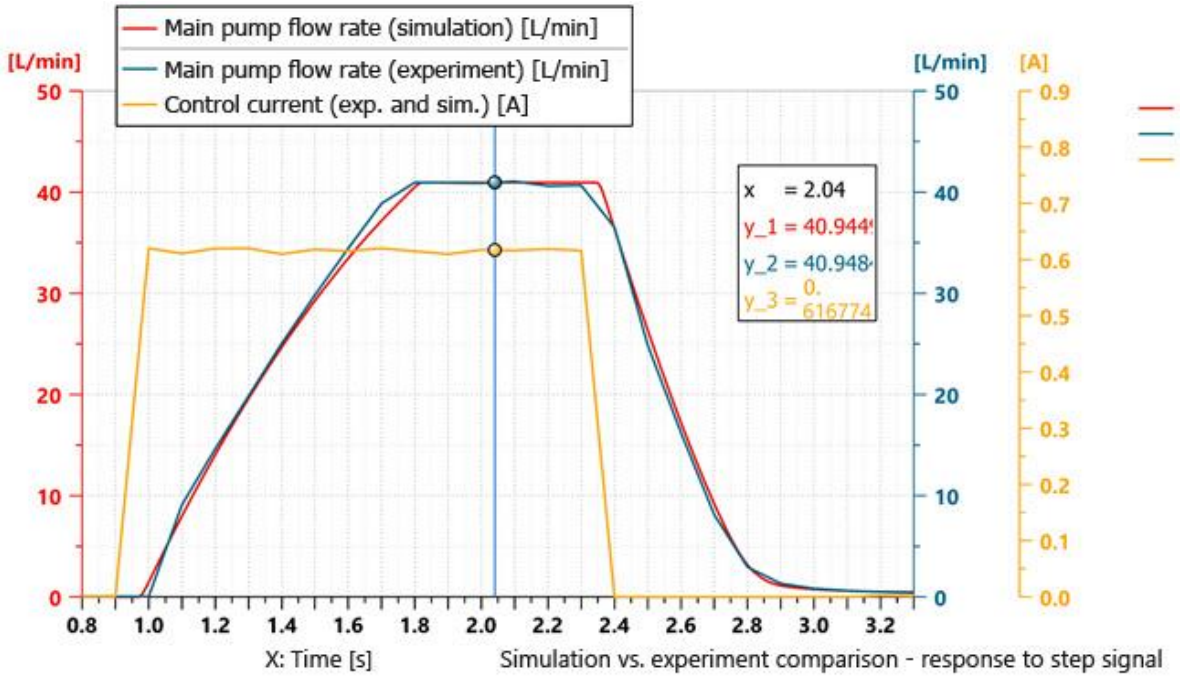

Fig. 14. Main pump flow rate and its control current – validation of numerical simulation

Flow rate/control characteristic of the servo-pump

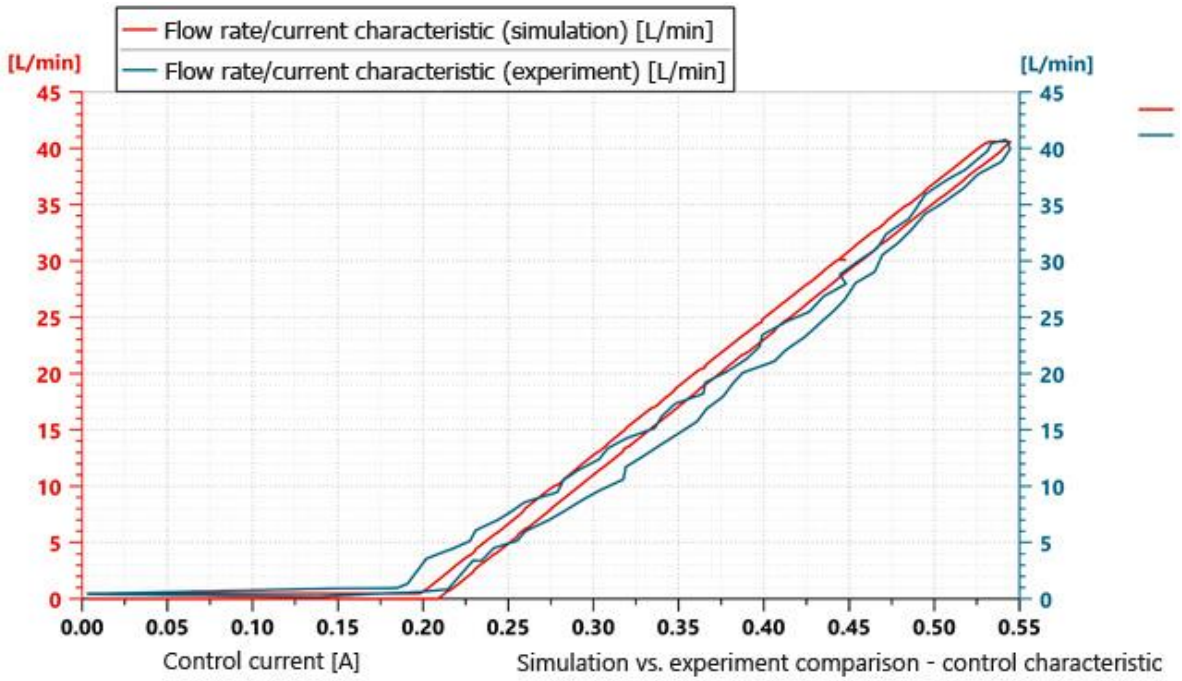

Fig. 15. Flow rate/control current characteristic – validation of numerical simulation results

In Fig. 15 one can see that the simulation results coincide with those of physical experimentation; the maximum flow rate is identical, and the current value from which the control of the pump displacement starts is similar; in this case, too, the control current is common.

The linear correlation coefficient

Fig. 16 estimates - as the name suggests - the linear correlation of two signals (physical parameters), in the present case, the linear correlation of the pump displacement control current, measured in amperes, and the servo-pump flow rate. A value of 0 or close to 0 of this coefficient indicates no linear correlation of the two signals, while a value close to 1, whether positive or negative, indicates a good linear correlation of the two signals.

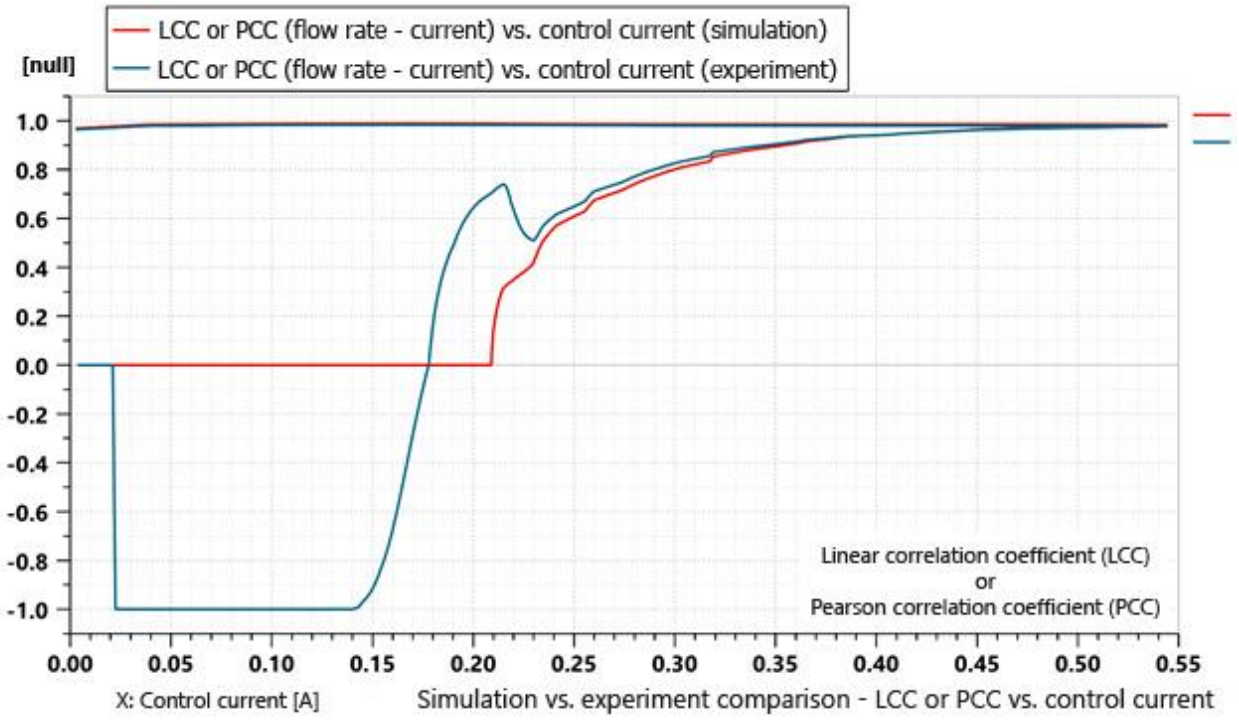

Fig. 16. Linear correlation coefficient - simulation vs. experimentation

The control current with which the displacement of servo-pumps for mobile applications is controlled has an insensitive "dead zone", in which the pump rate flow does not respond to the control signal, to avoid the alternate rectilinear movement of the motor truck when the swash plate of the servo-pump is in the neutral position and oscillates around it. In this case, the numerical simulation shows a superior linear correlation of the control current and the pump flow rate, because in simulation the conditions can be better controlled.

Frequency response of the servo-pump to the wobble control signal

The wobble control signal - constant amplitude and variable frequency control signal – is shown in Fig. 17 below.
Fig. 18 shows the time-variation of the servo-pump flow rate in response to the wobble control signal. This analysis is necessary for the correct tuning of the PID controller in the structure of the hydrostatic transmission of the motor truck.
Frequency response of the servo-pump flow rate is shown in Fig. 19 (Bode plot). On this graph, one can see what percentage of the flow rate amplitude is still available for a certain frequency, and also the phase shift. Comparing the results in this figure with the characteristics of the pump P7, one can see that the pump P7 achieves small amplitude flow rates at a maximum frequency of

17 Hz and a pressure of 70 bar, and the simulation reveals that the simulated servo-pump achieves small amplitude flow rates at 12 Hz, at a pressure of 20 bar.

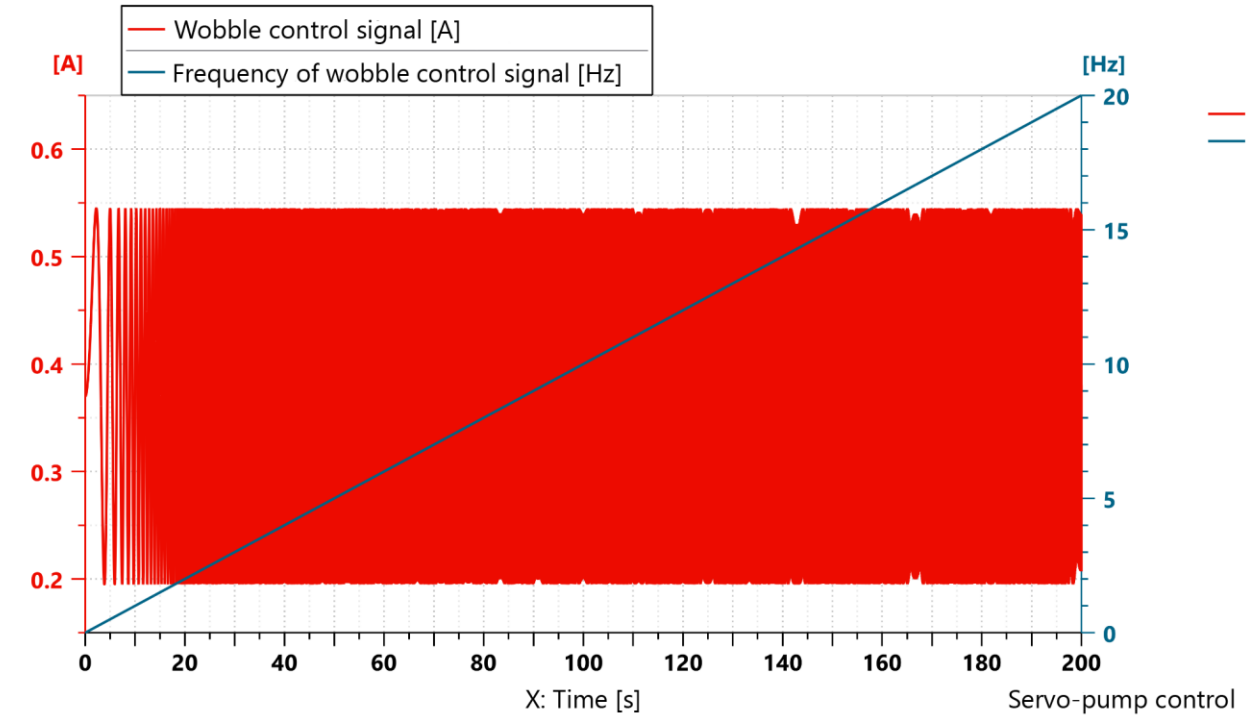

Fig. 17. Amplitude and frequency of wobble control signal

The influence of the wobble control signal on the flow rate of the servo-pump is shown in Fig. 18. On this figure one can see how, due to the increase in the frequency of the control signal, the amplitude of the servo-pump flow rate decreases. This attenuation of the flow rate amplitude can be counteracted by increasing the control pressure or by decreasing the mass of the components of the servo-control mechanism.

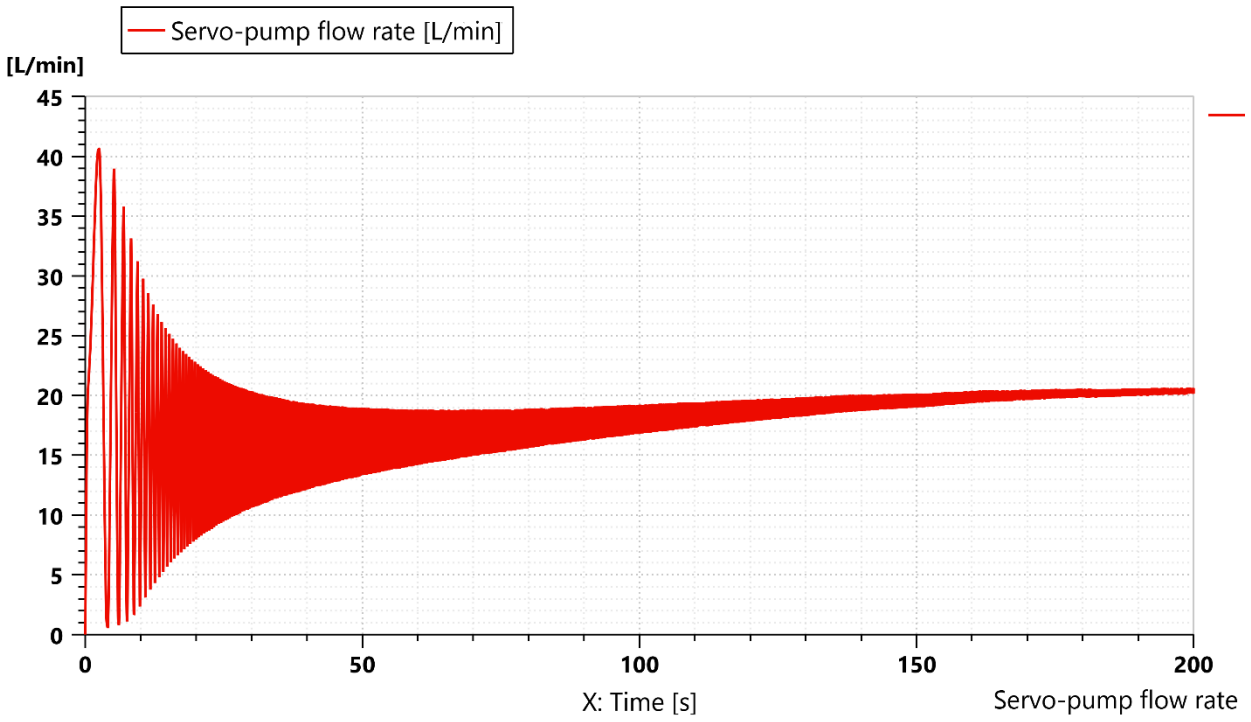

Fig. 18. Servo pump flow rate in response to wobble control signal

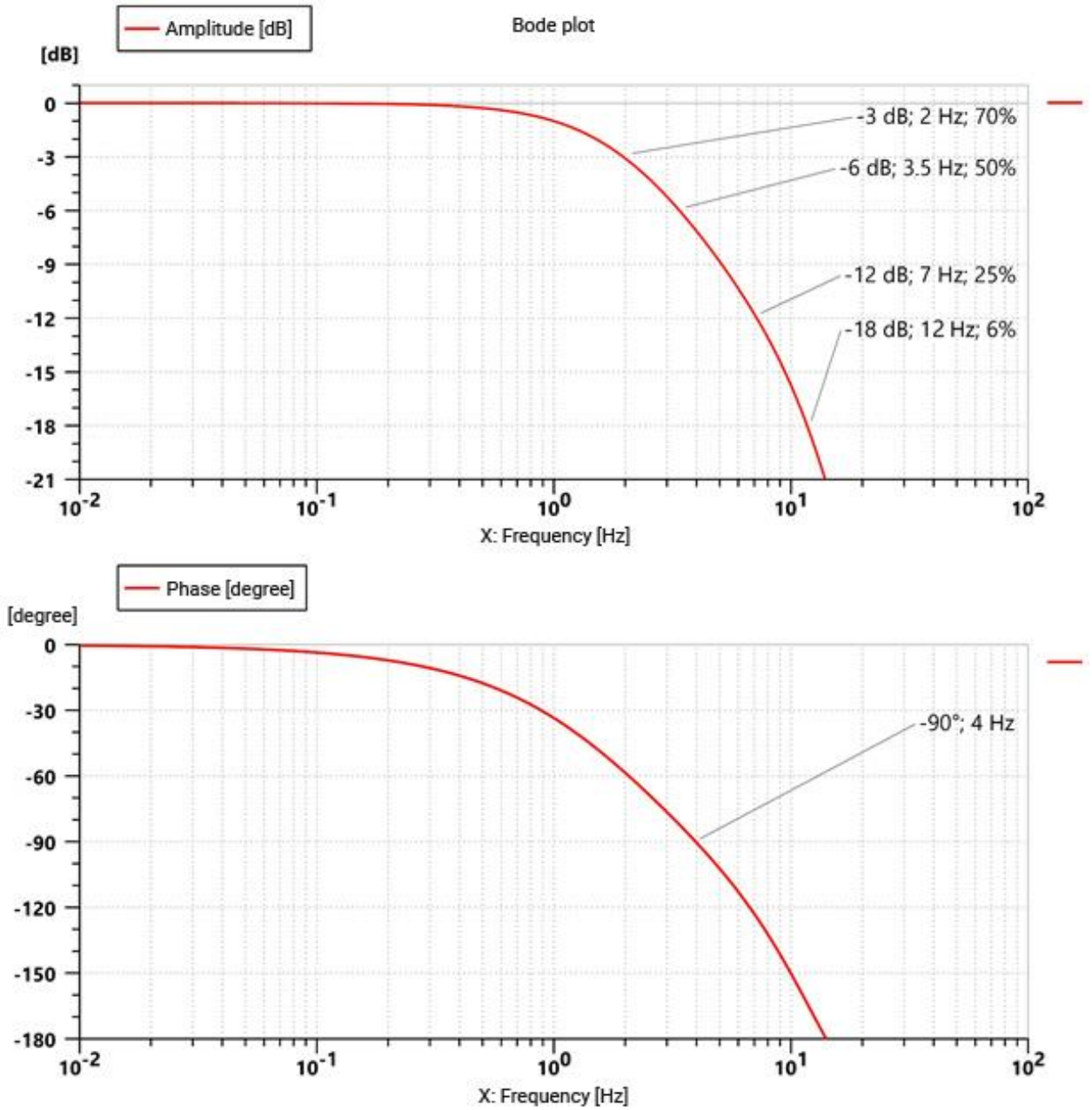

Fig. 19. Bode plot for frequency response of the servo-pump flow rate

4. Conclusions

- The time required for the servo-pump to reach maximum flow rate varies between 0.83 seconds and one second; it is measured between the time when the voltage control signal has been given and the time when the pump has reached maximum flow rate. If we exclude the time for processing the electrical signals from the calculation, one can see that the servo-pump reaches the maximum flow rate in 0.7 – 0.8 seconds. Regardless of the angle of the pump swash plate (0° or 33°) from which the voltage control is given, or of the load in the closed circuit, the servo-pump reaches maximum flow rate or 0 flow rate in no more than one second.
- The maximum theoretical flow rate of the servo-pump if it were to be driven at the synchronism speed of the asynchronous electric motor, is 42 l/min; two values have been determined experimentally, 40.77 l/min (with load) and 41.17 l/min (no load). The maximum flow rate of the servo-pump is load dependent: in proportion to the increase in pressure,

volumetric losses also increase. The flow rate of the servo-pump is also influenced by the variation of the speed rate of the asynchronous motor; this variation occurs as a result of the slippage between the stator and the rotor of the electric motor; this slippage is influenced by the resistive torque on its shaft; the torque is directly proportional to the pressure in the closed circuit.

- The minimum flow rate of the servo-pump is 0.116 l/min; it depends on the load since volumetric losses are proportional to pressure. The minimum flow rate is 0.2762% of the maximum theoretical flow rate of the servo-pump at a speed of 1500 rev/min, ($0.116/42 * 100 = 0.2762\ \%$).
- The pump flow rate becomes proportional to the control signals from the value of about 0.8 l/min, proportional adjustment starting from the voltage value of 1.1 volts and the control current value of 215 mA. The proportional relationship between the servo-pump flow rate and the control current is not significantly influenced by the load (pressure) in the closed circuit as long as the pump is operated at the nominal conditions specified by the manufacturer; the increase in pressure causes the increase in volumetric losses, and the latter reduce the flow rate for the same control current.
- Comparing the results of the numerical simulation with those determined experimentally, namely the response to the step signal and the control characteristic, it can be confidently stated that the numerical simulation model of the servo-mechanism controlling the displacement of the servo-pump is very similar to the one in the laboratory and can be used for further research.
- The previously mentioned conclusion is also strengthened by the strong linear correlation between the control signal and the flow rate of the servo-pump, both in the case of experimentation and in the case of numerical simulation.

Acknowledgments

The research presented in this article has been financed under a project funded by the Ministry of Research, Innovation and Digitalization through Programme 1- Development of the national research & development system, Sub-programme 1.2 - Institutional performance - Projects financing the R&D&I excellence, Financial Agreement no. 18PFE/30.12.2021.

References

[1] ASSOFLUID. *Hydraulics in Industrial and Mobile Applications*. Brugherio (Milano), Grafiche Parole Nuove s.r.l., 2007.
[2] Chapple, P. J. *Principles of Hydraulic System Design*. Oxford, Coxworth Publishing Company, 2003.
[3] Vasiliu, N., and I. Catană. *Hydraulic and electrohydraulic transmissions. Vol. I – Positive displacement hydraulic machines / Transmisii hidraulice şi electrohidraulice. Vol. I - Maşini hidraulice volumice*. Bucharest, Technical Publishing House, 1988.
[4] Merritt, H. E. *Hydraulic control systems*. New York, John Wiley & Sons, 1967.
[5] Stringer, J. *Hydraulic system analysis: an introduction*. Hoboken, John Wiley & Sons, 1976.
[6] Blackburn, J.F., G. Reethof, and J.L. Shearer. *Fluid power control*. Vols. 1, 2, and 3. New York & London, Technology press of M.I.T. and John Wiley & Sons, 1960.
[7] Manring, N. D., and G. R. Luecke. "Modeling and designing a hydrostatic transmission with a fixed-displacement motor." *Journal of Dynamic Systems, Measurement, and Control* 120 (1998): 45-49.
[8] Gies, H. M. S. *Fluid technology for mobile applications / Fluidtechnik für mobile anwendungen*. Aachen, Shaker Verlag, 2008.
[9] Costa, G. K., and N. Sepehri. *Hydrostatic transmissions and actuators: operation, modelling and applications*. West Sussex, John Wiley & Sons Inc., 2015.
[10] Zarotti, L. G., and R. Paoluzzi. "In quest of the transmission size." Paper presented at the Third JHPS International Symposium on Fluid Power, Yokohama, Japan, November 4 - 6, 1996.
[11] Wei, X., L. Wang, X. Ni, S. Han, X. Zhao, and S. Li. "Speed control strategy for pump-motor hydraulic transmission subsystem in hydro-mechanical continuously variable transmission." *Journal of Mechanical Science and Technology* 35, no. 12 (2021): 5665-5679.
[12] Axinti, G., and A. S. Axinti. *Hydraulic and pneumatic drives. Vol. 2. Dynamics of equipment and systems / Acționări hidraulice și pneumatice. Vol. 2. Dinamica echipamentelor şi sistemelor*. Chișinău, "Tehnica-Info" Publishing House, 2008.